Bulletin de l'Institut Scientifique, Rabat, section Sciences de la Terre, 2012, n° 34, p. 15-28.

Evidence of a Permian remagnetization in the Neoproterozoic-Cambrian Adoudounian Formation (Anti-Atlas, Morocco)

Florent BOUDZOUMOU[1,2], Didier VANDAMME[2], Pascal AFFATON[2]
Jérôme GATTACCECA[2], Hassane OUAZZANI[3], Lakhlifi BADRA[3]
& Elmahjoub MAHJOUBI[3]

1. *Université Marien Ngouabi, Faculté des Sciences, Département de Géologie, B.P. 69, Brazzaville, Congo.*
e-mail : florentboudzoumou@yahoo.fr
2. CEREGE, *Université d'Aix-Marseille, CNRS, B.P. 80, Europôle Méditerranéen de l'Arbois, 13545 Aix-en-Provence Cedex 04, France*.
3. *Université Moulay Ismail, Faculté des Sciences, Département de Géologie, B.P. 11201 Zaitoune, Meknès, Maroc*.

Abstract. A paleomagnetic study was undertaken on samples collected from seven sites of the exhumed and eroded Ait-Abdallah and Kerdous antiforms in the Moroccan Anti-Atlas of the West African craton. These sites are located in the Adoudounian Formation considered as of Neoproterozoic–Cambrian age. The magnetic mineralogy is represented essentially by magnetite and titanohematite. Magnetization is carried by three components respectively of high-temperature (500-670°C), medium-temperature (350-470°C) and low-temperature (NRM-300°C). Plotted in Gondwana Apparent Polar Wander Path, the high and medium temperature components close to the Permian pole and determine Permian overprint directions. The low temperature component closes to the present day field and corresponds to the present overprint day. This study shows that Permian overprint largely affect the Anti-Atlas area.

Key words: Paleomagnetism, Anti-Atlas, West-African craton, Adoudounian Formation, Neoproterozoic, Cambrian.

Mise en évidence d'une ré-aimantation permienne dans la Formation Adoudounienne, d'âge Néoprotérozoïque-Cambrien (Anti-Atlas, Maroc)

Résumé. Une étude paléomagnétique a été réalisée sur des échantillons provenant de 7 sites localisés dans les antiformes exhumés et érodés d'Ait Abdallah et de Kerdous dans l'Anti-Atlas au Maroc, et appartenant au craton ouest africain. Ces sites sont situés dans la Formation Adoudounienne d'âge Néoprotérozoïque-Cambrien. La minéralogie magnétique est représentée essentiellement par la magnétite et la titano-hématite. L'aimantation est portée par trois composantes respectivement de haute température (500-670°C), moyenne température (350-470°C) et basse température (NRM-300°C). Placées dans la courbe de la dérive apparente du pôle du Gondwana, les composantes de haute et moyenne températures se placent à proximité des pôles permiens et caractérisent les directions des réaimantations permiennes. La composante de basse température se situe au niveau du champ actuel et correspond à la ré-aimantation de ce champ. Cette étude montre que la ré-aimantation permienne affecte largement la région de l'Anti-Atlas.

Mots clés : Paléomagnétisme, Anti-Atlas, Craton ouest africain, Formation de l'Adoudounien, Néoprotérozoïque, Cambrien.

INTRODUCTION

The Anti-Atlas is situated in the northwestern extremity of the West-African craton. It is a WSW-ENE oriented mountain chain of about 600 km, characterized by a Paleoproterozoic basement complex that is overlain by Neoproterozoic to Paleozoic cover sequences (Fig. 1). The basement crops out as exhumed antiforms (the *Boutonnières*) that have been exposed by post-Hercynian erosion.

The Anti-Atlas, like the other parts of the West-African craton, is characterized by a sparse paleomagnetic database for the Neoproterozoic to Cambrian interval. The available Neoproterozoic and Cambrian data are often considered to be representative of remagnetization in the Permian (Tohver *et al.* 2006, Font *et al.* 2012). On the West-African craton, only the Neoproterozoic poles of the Adma diorite, located in the Adrar of Iforas (Morel 1981), and the Paleozoic Hasi-Messaud sediments are considered reliable and used in the reconstruction of the Apparent Polar Wander Path (APWP) of the West-African craton (Tohver *et al.* 2006), although the last pole is not considered robust and not used in the Gondwana APWP of Trindade *et al.* (2006) and of Font *et al.* (2012) in which more poles are presented.

This study is based on 73 samples collected in the Adoudounian Formation from the Ait-Abdallah, Ida Ougnidif, Douar Tizirt and Anfeg areas (Fig. 1). The Adoudounian Formation studied in different localities yielded a U-Pb zircon age of between 550±3 Ma and 521±7 Ma (Gasquet *et al.* 2005), 534 ± 10 Ma (Alvaro *et al.* 2006) and 524.84 ± 0.09 Ma (Maloof *et al.* 2010). It was folded during the Hercynian orogeny in 2 phases, dated by Rb-Sr and K-Ar methods on fine illite fractions at around 315-250 Ma (Charlot 1976), 370-290 Ma (Bonhomme & Hassenforder 1985), and at 328±30 Ma (Sebti *et al.* 2009).

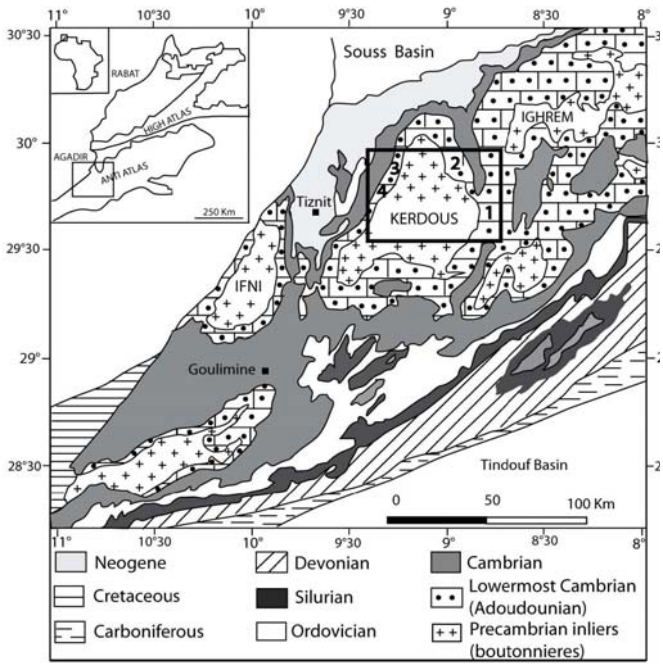

Figure 1. Geological map of the Western Anti-Atlas (Gasquet *et al.* 2004) and location of the studied sites: 1, Ait-Abdallah 1- 4; 2, Douar Tizirt; 3, Ida Ougnidif; 4, Anfeg.

GEOLOGY OF THE WESTERN ANTI-ATLAS

The western part of the Anti-Atlas is underlain by a Paleoproterozoic basement complex that is capped by Neoproterozoic volcano-sedimentary cover sequences and a mostly Paleozoic sedimentary cover (Fig. 2). The Neoproterozoic units are partially affected by the Pan-African orogeny and were refolded during the Hercynian orogeny. The Paleozoic cover was only affected by the latter.

The basement is composed of a polymetamorphic complex of gneisses, amphibolites and micaschists, together with Paleoproterozoic and Pan-African mafic intrusives and granitoids (Malek *et al.* 1998, Mortaji *et al.* 2000, Barbey *et al.* 2004). The Pan-African intrusives include diorites, gabbros, granodiorites, monzonites and granites. The basement was metamorphosed during the Eburnean (Thomas *et al.* 2002).

The cover sequences, of about 13 km in thickness (Gasquet *et al.* 2005), consist of two unconformable megasequences that are Neoproterozoic and Paleozoic in age, respectively. The Neoproterozoic megasequence starts with the Anti-Atlas Supergroup (Gasquet *et al.* 2005). It comprises platform marine sedimentary sequences with continental affinity, mainly composed of conglomerates, quartzite, greywackes, sandstones, shales, silexites, stromatolitic limestones; volcanic rocks consist of ignimbrites, andesites, cinerites, spilites and keratophyres. The assemblage is associated with an ophiolitic complex made up of basic and ultra-basic rocks and intrusions of quartz-diorite. The volcano-sedimentary Ouarzazate Supergroup lies with an erosional unconformity on the lower supergroup and crops out widely around the old massifs of the Anti-Atlas (i.e. the Bou Azzer and Kerdous areas) and the exhumed anticlines of Bas Dra and Ifni. It consists of about 1 km-thick dacitic to rhyolitic ignimbrites, andesitic and basic lava flows, conglomerates and sandstones (Gasquet *et al.* 2005). Two magmatic episodes occurred at 595-570 Ma and 570-545 Ma respectively (Gasquet *et al.* 2005). The Neoproterozoic cover is affected by a Pan-African phase of deformation considered to be 579 ± 1.2 Ma, i.e. age of the undeformed intrusive Bleida granodiorite (Inglis *et al.* 2004).

The Adoudounian Formation overlies the Ouarzazate Supergroup with an unconformably/para-unconformably deeply dissected or angular discordance of up to 20° (Thomas *et al.* 2002). It is about 2 km-thick and composed of conglomerates, microconglomeratic sandstones, coarse grained and fine- to medium- grained sandstones, shales, limestones including stromatolitic dolomites and intercalations of alkaline olivine basalts, trachytes, and andesites. Upwards, the Lie-de-Vin Formation consists of shales, siltstones, fine- to medium-grained sandstones and micro-conglomeratic sandstones. The Adoudounian Formation yielded U-Pb zircon age of between 550±3 Ma and 521±7 Ma (Gasquet *et al.* 2005), 534 ± 10 Ma (Alvaro *et al.* 2006) and 524.84 ± 0.09 Ma (Maloof *et al.* 2010).

The Paleozoic megasequence is of Cambrian to Carboniferous age and composed of carbonate, siliciclastic and chemical sedimentary units with a rich fossil fauna. It will not be considered further.

PALEOMAGNETISM

Seven sites of the Adoudounian Formation were sampled around the exhumed Kerdous antiform. These sites are named Ait-Abdallah 1, 2, 3 and 4, Ida Ougnidif, Douar Tizirt and Anfeg (Fig. 1). Seventy-three core samples were processed in the Geophysics and Planetology laboratory at the CEREGE, France.

Materials and method

In the exhumed Ait-Abdallah anticline, the samples are collected from an asymmetric anticline located in the lower part of the Adoudounian. The sides are made of a succession of limestone and siltstone beds. The Ait-Abdallah sites 1 and 2 are located on the eastern side while the Ait-Abdallah sites 3 and 4 are located on the western side.

Samples were collected using a portable gasoline powered drill, and subsequently oriented with magnetic and sun compass. They were cut into cylindrical specimens (2.5×2.3 cm) and stored in a non-magnetic chamber in which magnetic measurements were also undertaken. Sample lithologies are represented by grey to pink limestones and reddish siltstones. They were subjected to thermal demagnetization in order to isolate their Characteristic Remanent Magnetization (ChRM). Thermal

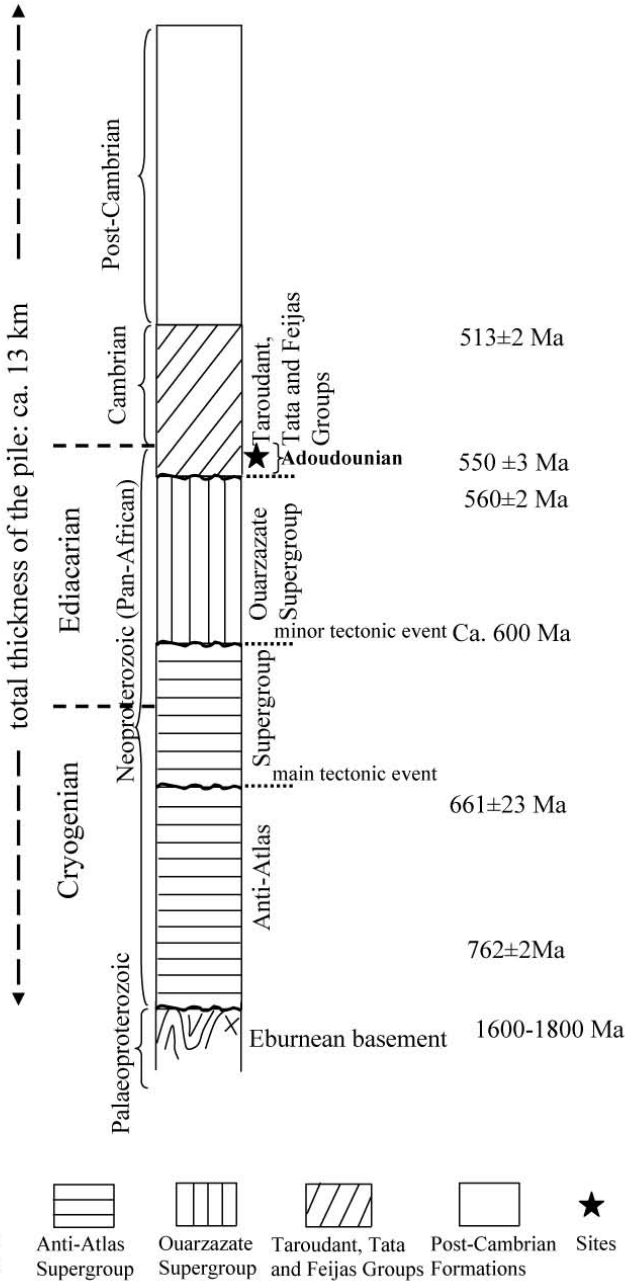

Figure 2. Simplified lithostratigraphy of the Anti-Atlas, after Gasquet *et al*. (2005).

demagnetization was done using a CEREGE furnace with sixteen heating steps (120, 200, 250, 300, 350, 400, 440, 470, 500, 525, 550, 575, 600, 625, 650 and 670°C). Remanence measurements were done using a SQUID (2G Enterprises) cryogenic magnetometer.

The determination of the remanence carriers was done by three methods:

(1) Analyses of thermomagnetic curves for powders samples using a Multifunction Kappa bridge (MFKCSI) under an Argon atmosphere in order to limit chemical alteration during heating.

(2) The Lowrie's (1990) test, which consists of measuring magnetization by progressive thermal demagnetization of three Isothermal Remanent Magnetizations (IRM) applied on three orthogonal axes of the sample, with fields of 3 T, 0.4 T and 0.12 T respectively. IRM acquisition was done using a field pulse magnetizer (MMPMQ).

(3) Hysteresis curves were produced for the samples using a Micromag vibrating sample magnetometer (maximum field 1 T).

The ChRM directions were determined by the principal components analysis (Kirschvink 1980). The mean principal directions at each site were calculated using Fisher (1953) statistics. Data processing was done with Cogne's

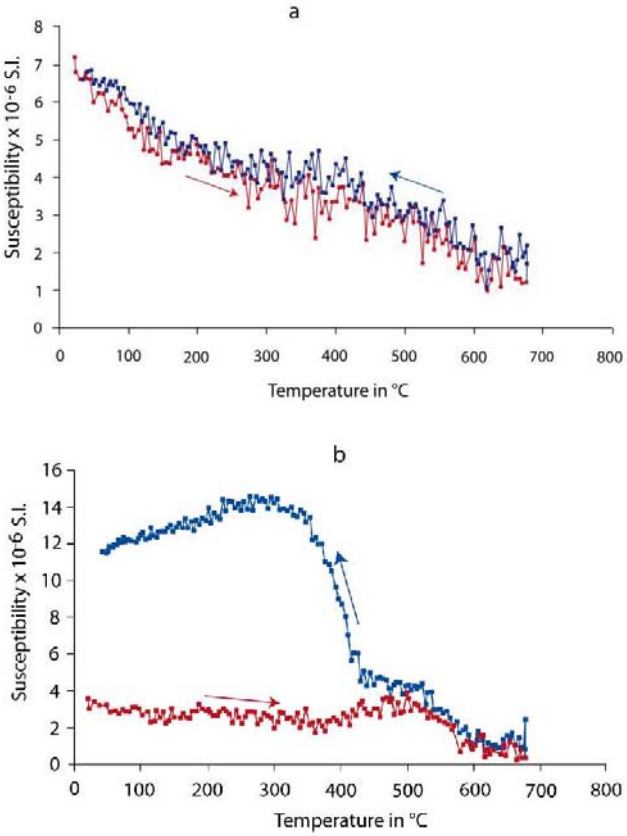

Figure 3. Example of thermomagnetic curves: a, Ait-Abdallah 02-05; b, Ait-Abdallah 04-03. Red: heating curve; blue: cooling curve.

(2003) Paleomac 6.1 software. Sampling allowed for a McFadden (1990) fold test for an anticline of the Ait-Abdallah sites 2 and 4 which has the potential fold test to constrain the relative age of the remanence acquisition.

Results

Magnetic mineralogy

Powdered specimens were processed under an argon tmosphere and heated to temperatures of up to 670 °C and then cooled down to room temperature. The curves (Fig. 3) obtained were either reversible (Fig. 3a) or irreversible (Fig. 3b). Irreversible curves show a slight increase of the heating curve from 400 to 500ºC (Hopkinson effect?) and an abrupt decrease at 580ºC indicating presence of Ti-poor magnetite. Above 580ºC, data are noisy. The cooling curve is mostly reversible until ~500ºC where a increase in MS is observed and due to formation of secondary iron-oxides during heating. The decline in susceptibility takes place at temperatures close to 575°C and to 675°C; characteristic of magnetite and titanohematite respectively.

Lowrie's (1990) test was performed on 13 samples. The results are very heterogeneous. The highest intensity is carried by the hard fraction in some carbonate (Fig. 4 a, b) or by medium to high fraction (Fig. 4c) in some siltstones.

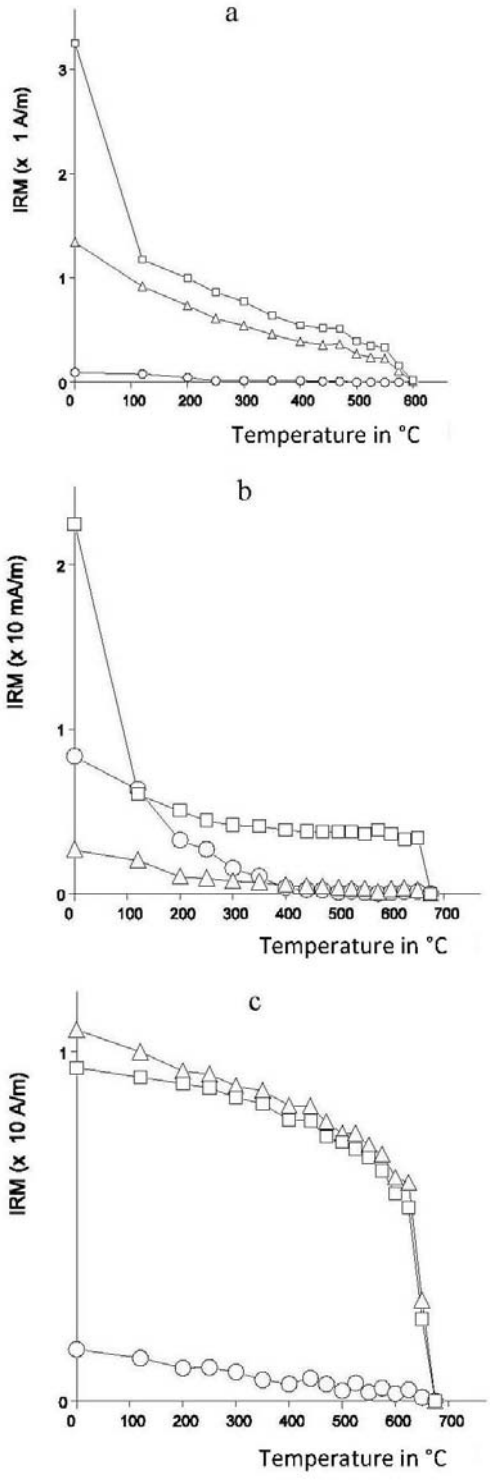

Figure 4. Example of thermal demagnetization of three axes of Isothermal Remanent Magnetization according to Lowrie's (1990) method applied to some samples from the Anti-Atlas. Squares: Hard fraction; triangles: Medium fraction, circles: Soft fraction. (a) AA03-10B: Ait Abdallah carbonate; (b) DT 01-05: Douar Tizirt carbonate; (c) ID02: Ida Ougnidif siltstone.

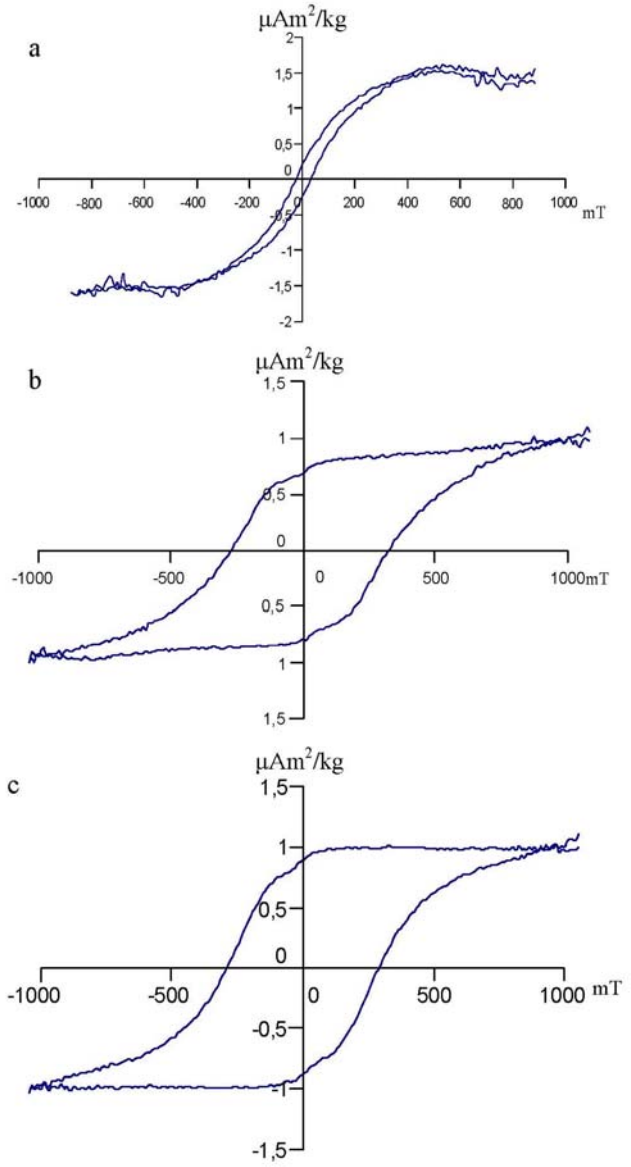

Figure 5. Hysteretic curves with sample dip correction: a, Ait-Abdallah 2 – 04 siltstone; b, Ida Ougnidif 2 siltstone; c, Ida Ougnidif 3 siltstone.

These heterogeneities are also described in the Volta and Taoudeni basins (Boudzoumou *et al.* 2010, 2011) where the highest intensity is carried by these different fractions just as well in the carbonate or in the siltstone. The hard and medium fractions, in the carbonate sample AA03-10B of Ait Abdallah site 3 (Fig. 4a), show unblocking temperature at 575°C determining the presence of the magnetite. In the carbonate sample DT 01-05 of Douar Tizirt (Fig. 4b), the hard fraction shows unblocking temperature at 675°C corresponding at the presence of the titanohematite and the medium and soft fraction shows unblocking temperature around 575°C corresponding to the presence of the magnetite. In the two samples a strong decrease of the harder fraction at around 100ºC is indicative of the presence of goethite probably coming from the hydroxidation of original hematite. In the siltstone sample ID 02 of the Ida Ougnidif site, although the high intensity curve is carried by the medium fraction, it is not very different from the hard fraction intensity. The two fractions remain bonded or coupled until the total destruction of magnetization at 675°C. This behaviour could indicate the presence of titanohematite. In conclusion, the Lowrie's (1990) test shows the presence in the samples of either magnetite or titanohematite respectively or a mixture of the two minerals.

.

Hysteresis loops were obtained for 10 siltstone samples from Ait-Abdallah sites 2 and 4 and from the Ida Ougnidif site. Each specimen was subjected to a field of 1 T in order to saturate the magnetic minerals. The curves were then corrected for slope. Specimen AA02-04 from siltstones shows curves (Fig. 5a) with narrow spacing, characteristic of Pseudo-Single-Domain (Tauxe 2009) and associated values Bcr/Bc = 0.15, Mrs/Ms= 3.97 corresponding to magnetic grains of the Pseudo-Single-Domain (Day *et al.* 1977). The specimens from the siltstone of the Ida Ougnidif (Fig. 5,b,c) display wide open shape which do not saturate until 1000 mT. This is indicative of the presence of ferromagnetic grains such as titanohematite which is observed in the Lowrie's (1990) test.

To summarize, the magnetic mineralogy of our samples is composed of magnetite and titanohematite, the latter being dominant in the siltstones at the Ait-Abdallah sites 2 and 4 as well as in those at the Ida Ougnidif site.

Paleomagnetic data

The samples carry a Natural Remanent Magnetization (NRM) with variable intensity between 9×10^{-5} and 2×10^{-2} A/m. The average intensity at each site is indicated in Table I. Kirschvink's (1980) principal components were deduced from linear segments on Zijderveld's (1967) orthogonal projections from thermal demagnetization data and forced to the origin. Circle methods were also used but did not provide reliable results compared to line-fits. Depending on samples, one to three components were detected, namely a low (NRM at 300°C), a medium (350°C to 470°C) and a high (500°C to 670°C) temperature magnetic component (Fig. 6).

Mean magnetic components were calculated from high-temperature (500 to 575°C or 500 to 670°C) and medium-temperature (350-470°C) components based on in situ and tilt corrected directions (Table I, Figs. 7-9). Limestones showed distinct magnetic records from that of siltstones.

The Ait-Abdallah sites 1 and 3 are in grey to pink fine limestone horizons and are plotted in figures 7a-h. Depending on the sample, the high-temperature component is carried either by magnetite, or by a mixture of magnetite and titanohematite. Site-mean magnetic component were calculated based on in situ and tilt corrected direction (Tab. I). The site-mean high-temperature magnetic component of Ait-Abdallah site 1 (Fig. 7a,b) shows higher precision parameter (k) after tilt correction (k_2 = 440.7) than in situ (k_1 = 147.1). The negative McFadden (1990) fold test indicates a post folding magnetization. In the Ait-Abdallah site 3 (Fig. 7c,d), precision parameters (k) in situ (k_1 = 71.9)

Table I. Mean directions of the high-temperature components at Ait-Abdallah 1-4, Anfeg, Douar Tizirt and Ida Ougnidif sites, and medium-temperature components at sites Ait-Abdallah 2 and 4 and Ida Ougnidif. N: number of samples used in Fisher's calculation; n: number of samples processed; Jr: Natural Remanent Magnetization; Mx: dominant magnetic minerals (m=magnetite; th= titanohematite) ; D and I: declination and inclination; *k*: Precision Parameter; α_{95}: Semi angle of the 95% confidence cone; dp/dm: 95% confidence semi axes; Paleol: Paleolatitude.

Sites	N/n	Jr (10^{-3}A/m)	Mx	in situ				after tilt correction				South Virtual Geomagnetic Pole						Paleol
												in situ		after tilt correction				
				D	I	k	α_{95}	D	I	*k*	α_{95}	Lon	Lat	Lon	Lat	dp	dm	
High-temperature component																		
Ait Abdallah 1	4/11		m, th	343.1	27.4	147.1	7.6	325.7	4.7	440.7	4.4	42.3	–68.7	48.9	–47.8	2.2	4.4	2.4
Ait Abdallah 3	6/9		m, th	339.1	29.5	71.9	8.0	347.7	–0.6	78.6	7.6	51.8	–66.6	15.8	–58.3	3.8	7.6	–.3
Mean Ait Abdallah 1-3	10/20	0.37		340.7	28.7	93.5	5.0	338.9	1.6	35.2	8.3	48.1	–67.5	31.1	–55.2	4.1	8.3	0.8
Ait Abdallah 2	5/10			111.8	35.1	13.9	21.3	93.1	12.3	15.2	20.2	54.1	–8.4	74.9	0.4	10.5	20.6	6.2
Ait Abdallah 4	4/8			333.4	71.6	6.8	37.9	278.0	7.6	8.6	33.2	144.8	–56.9	81.3	–8.9	16.8	33.5	56.3
Mean Ait Abdallah 2-4	9/18	1.65	th	120.9	–8.0	1.9	52.9	95.2	3.6	10.8	16.4	69.5	–28.8	77.7	–3.7	8.2	16.5	1.8
Ida Ougnidif	10/12	5.05	th	95.1	31.7	13.2	13.8	93.8	25.9	12.2	14.4	63.6	4.1	67.3	3.4	8.4	15.6	13.6
Anfeg	5/11	1.19	m	9.0	29.2	31.9	13.8	6.3	38.3	40.5	12.2	137.4	74.1	132.7	80.5	8.4	15.2	15.6
Douar Tizirt	6/12	0.63	m, th	3.8	33.9	22.1	14.6	4.3	24.0	17.9	16.3	152.0	78.9	156.7	72.9	9.5	16.7	18.6
Medium-temperature component																		
Ait Abdallah 2	10/10			125.9	11.1	148.3	4.0	119.0	4.6	66.3	6.0							
Ait Abdallah 4	7/8			120.7	14.3	28.4	11.5	173.9	52.2	40.7	9.6							
Mean Ait Abdallah 2-4	17/18			123.8	12.4	54.4	4.9	134.6	26	5.6	16.5	57.6	–25.3	43.5	–28.5			
Ida Ougnidif	10/12			133.2	14.1	54.9	6.6	131.7	1.8	51.1	6.8	49.5	–32.0	51.7	–31.6			
Mean Abdallah- IdaOugnidif	27/30			127.3	13.1	48.2	4.8	133.4	20.2	8.0	10.4	54.5	–28.0	46.7	–30.1	5.7	10.9	6.6

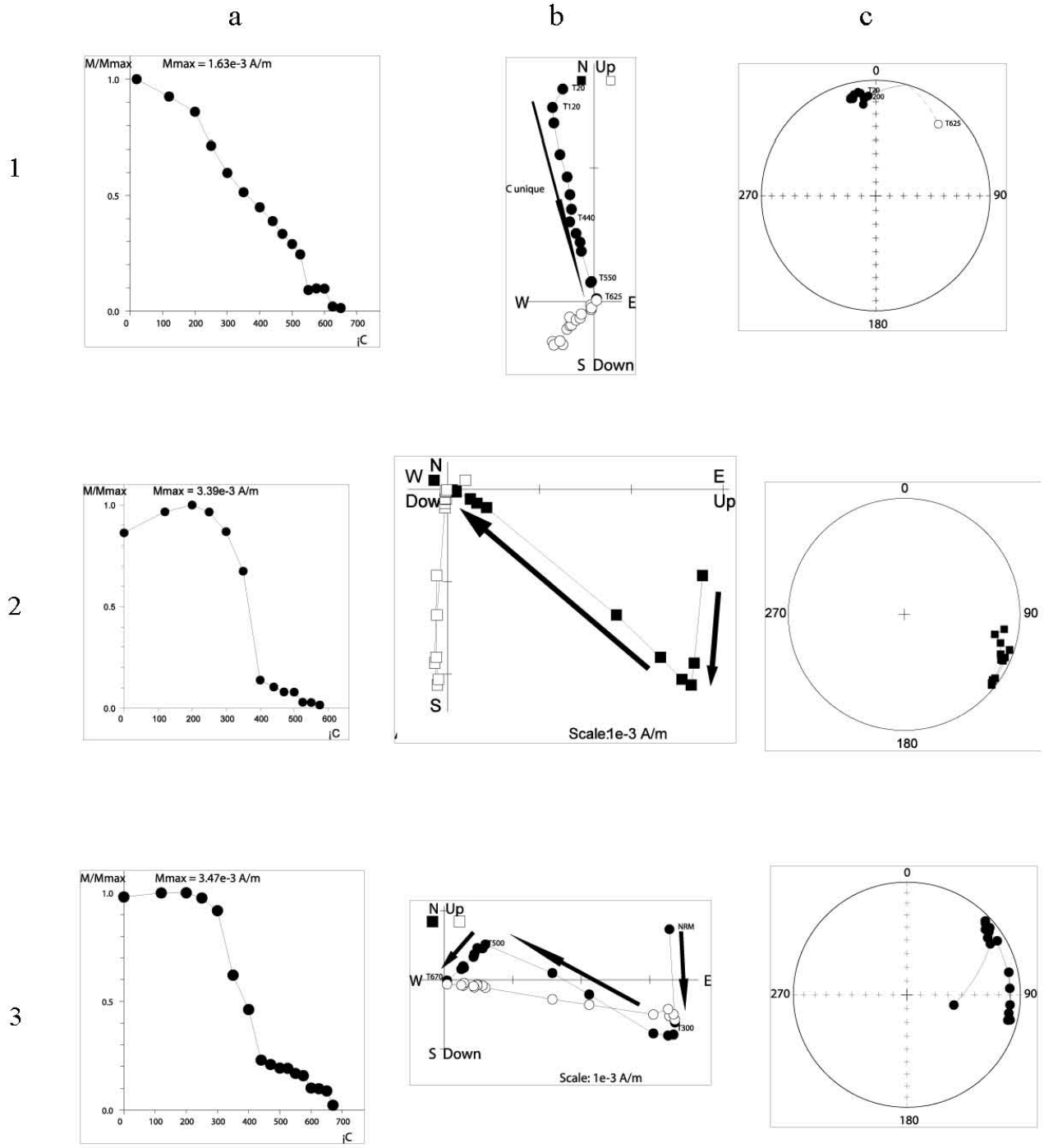

Figure 6. Thermal demagnetization of characteristic samples from Douar Tizirt and Ait Abdallah 2. 1- Sample DT01-01. 2- Sample AA02-09. 3- Sample AA02-07A. a, intensity curves as a function of temperature; b, Zijderveld's diagrams (open circles = vertical projection of vector data; closed symbol = horizontal projection of vector data), 1b shows one component, 2b shows two components and 3b shows three components (CBT- lower-temperature component, CMT- medium-temperature component, CHT- high-temperature component); c, stereographic projections of demagnetization data after tilt correction (the open/full circles correspond to projections on the vertical/horizontal plane)

and after tilt correction (k_2 = 78.6) are both enough close. Considering that both sides were tabular before folding, the mean direction was calculated after mean sample-mean direction of sites 1 and 3 in order to perform a fold test. Results (Fig. 7e,f) give a mean component at D=340.7° and I=28.7° (k_1=93.5, α_{95}=5.0°) in situ, and at D=339.9°, I=1.6° (k_2=35.2, α_{95}=8.3°) after tilt correction. The precision parameter k_1 for in situ directions is largely higher than k_2 after tilt correction. For in situ directions, site-mean directions are indistinguishable from the expected direction of the Present-day field at the sampling site. In situ medium-temperature components (Fig. 7g) cluster into two

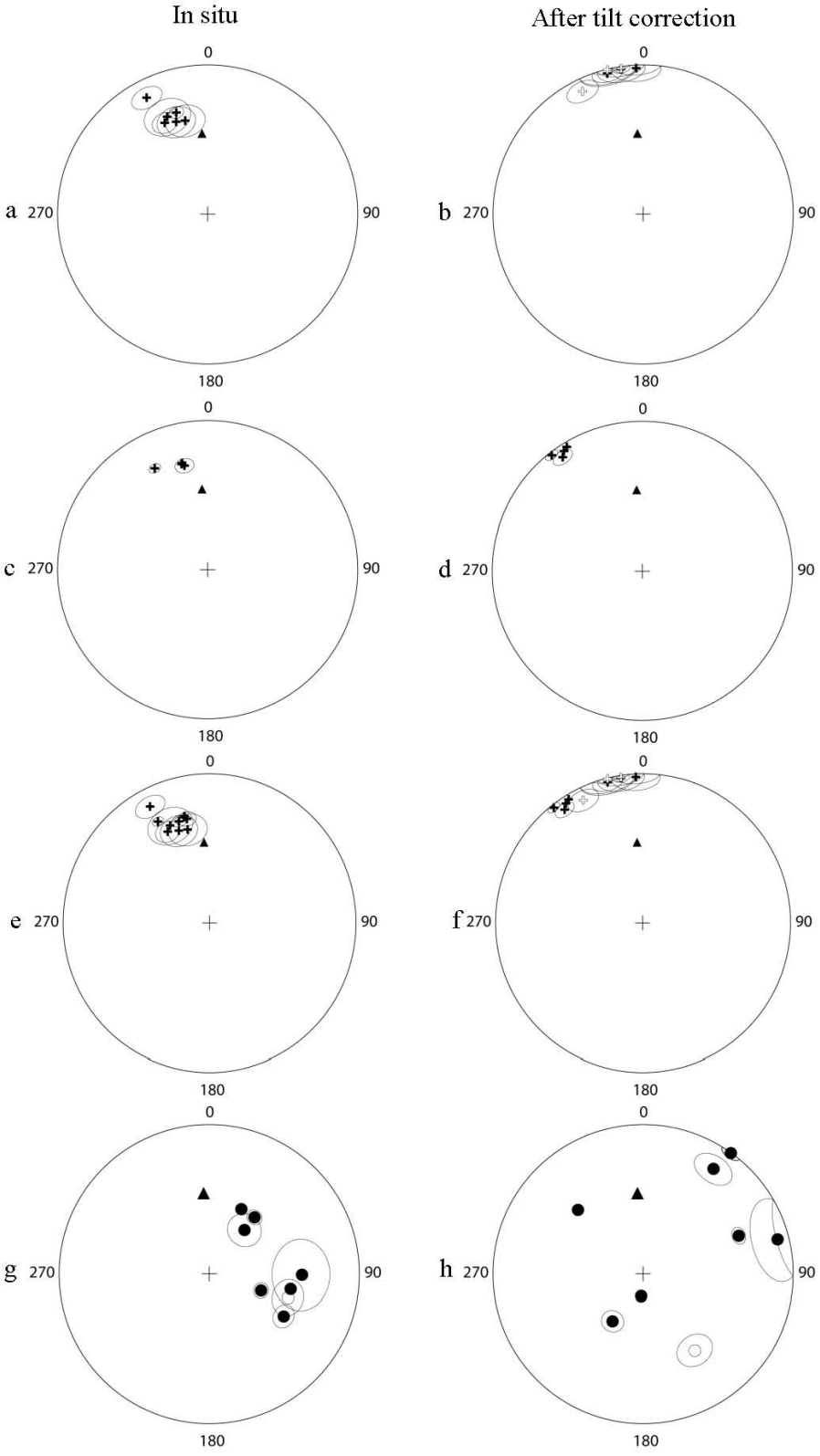

Figure 7. Stereogram of sample-mean directions, in situ and after tilt correction, showing the high (+) and medium (●) temperature-components. (▲) current geomagnetic field. Sites: a, b, Ait-Abdallah 1; c, d, Ait-Abdallah 3; e, f, Mean of Ait-Abdallah 1 and 3; g, h-Medium-temperature component of Ait-Abdallah 1 and 3. The high-temperature component better clusters after tilt correction but disperses after meaning sites 1 and 3. The medium-temperature component better clusters when considering in situ rather than tilt corrected directions.

,

groups, directed easterly and north-easterly. After tilt correction, data are more scattered also suggesting a post-folding origin for the magnetization (Fig. 7h).

The Ait-Abdallah sites 2 and 4 are located in the reddish siltstone horizons and plotted in figure 8. The high-temperature component is carried by titanohematite (Fig. 4c) or by mixture of magnetite and titanohematite (Figs. 3-5). Site-mean directions are reported in Table I. The high-temperature component of Ait Abdallah site 2 (Fig. 8a,b) give mean direction in-situ at D=111.8° and I=35.1° (k_1=13.9, α_{95}=21.3°) and after tilt correction at D=93.1° and I= 12.3° (k_2=15.2, α_{95}=20.2°). The mean direction in Ait Abdallah site 4 (Fig. 8c,d) is in-situ D= 333.4° and I=71.6° (k_1=6.8, α_{95}=37.9°) and after tilt correction D=278.0° and I=7.6° (k_2=8.6, α_{95}=33.2°). Similarly to the Ait-Abdallah sites 1 and 3, the mean in situ and tilt corrected direction after meaning both sites in the same hemisphere (Fig. 8e,f) give a mean component located at D= 120.9° and I=-8.0° (k_1=1.9, α_{95}=52.9°) and D= 95.6° and I= 3.6° (k_2=10.8, α_{95}=16.4°) respectively. This direction (Fig. 8f) gives a positive response to the fold test of Mcfadden (1990). Unfortunately this positive fold test is supported by very low quantity of samples processed and could not be significant. This high-temperature component is considered post folding.

The high-temperature component direction in the Ait Abdallah sites 2 and 4 (Fig. 8e, f) is different from the low (Fig. 8g, h) and medium-temperature (Fig. 8i,j) component directions. The low-temperature component shows a direction D=345.2°, I=38.3° (k_1=67.1, α_{95}=4.4°) for in situ directions, and D=336.3°, I=2.1° (k_2=8.5, α_{95}=13.8°) for tilt corrected directions. This value is close to the current field and clearly fails the fold test. The direction of the medium-temperature component located in the SE quadrant (Fig. 8 i,j Tab. I) is D=123.8° and I= 12.4 (k_1=54.4, α_{95}= 4.9°) in-situ and D=134.6° and I= 26 (k_2= 5.6, α_{95}= 16.5°) after tilt correction. The precision parameters (k), which are higher in situ than in tilt-correction, attribute this direction to remagnetization.

In conclusion, the three (high, medium and low temperature) components bear a remagnetization direction.

The Ida Ougnidif site is composed of reddish siltstones. As in the case of the Ait-Abdallah 2 and 4 siltstones, three components are determined. The high-temperature component (Fig. 9a, b) is carried by titanohematite and shows a direction D=95.1° and I=31.7° (k_1=13.2, α_{95}=13.8°) in situ and D=93.8° and I=25.9° (k_2=12.2, α_{95}=14.4°) after tilt correction. This easterly direction is also present in siltstones from Ait-Abdallah site 2 as well as medium-temperature components from limestones from Ait-Abdallah site 1-3 (Fig. 7g) and is attributed to Permian overprint. The low-temperature component has a direction of D=355.8° and I=35.1° (k_1=37.1, α_{95}=10°) in situ and D=359.9° and I=33° (k_2=45.7, α_{95}=9°) after tilt correction. This direction is close to the present-day field. The medium-temperature component (Fig. 9c,d, Tab. I) shows a direction D=133.2° and I=14.1° (k_1=54.9, α_{95}=6.6°) in-situ and D=131.7° and I=11.8° (k_2=51.1, α_{95}=6.8°) after tilt-correction. This direction is located in SE quadrant similarly to the Ait Abdallah 2 and 4 sites and is attributed to the Permian remagnetization.

The Anfeg site is located in limestones. The high-temperature component is carried either by magnetite or by titanohematite. It shows an average direction close to the present field (Fig. 9e,f, Tab. I). The low and medium-temperature components are scattered and do not provide reliable results.

The Douar Tizirt site is located in limestones. The high-temperature component has an average direction close to the present field (Fig. 9g, h, Tab. I). Like the Anfeg site, the low and medium-temperature components are completely scattered.

Limestone and siltstone samples of the Adoudounian Formation are characterized by three distinct remanence directions determined by three components respectively of low (NRM-300°C), medium (350°-470°C) and high (500°-670°) temperatures magnetic component (Fig. 6). Based on the comparison on the precision parameters (k) of each magnetic direction in situ and after tilt-correction, the three components are interpreted as overprint directions. Siltstones record a modern overprint that is revealed after low temperature demagnetization. The same overprint is revealed in limestone samples but it is persistent up to high temperatures. Siltstone samples record a shallow southeasterly magnetization (revealed by medium temperature demagnetization steps) that clearly postdates folding. A third component is revealed in most cases by high-temperature demagnetization steps and within siltstone samples. These high-temperature components are easterly and upward.

The high and medium temperature magnetization are linked to the Hercynian tectonics which affects the Anti-Atlas and dated by Rb-Sr and K-Ar methods on fine illite fractions at around 315-250 Ma (Charlot 1976), 370-290 Ma (Bonhomme & Hassenforder 1985), and at 328±30 Ma (Sebti *et al.* 2009).

DISCUSSION

The studied sites are located in the Adoudounian Formation dated by U-Pb zircon between 550±3 Ma and 521±7 Ma (Gasquet *et al.* 2005), 534 ± 10 Ma (Alvaro *et al.* 2006) and 524.84 ± 0.09 Ma (Maloof *et al.* 2010). It was folded during the Hercynian in 2 phases, dated by Rb-Sr and K-Ar methods on fine illite fractions at around 315-250 Ma (Charlot 1976), 370-290 Ma (Bonhomme & Hassenforder 1985), and at 328±30 Ma (Sebti *et al.* 2009).

The sites are made of limestones and siltstones and provide three remanence directions detected in low medium and high temperatures respectively. The low-temperature (NRM-300°C) component is clearly similar to the present-day field (Fig. 8e). The medium- temperature components (350°C to 470°C) (Fig. 8g, h) of Ait Abdallah 2 and 4 shows an in situ precision parameter (k_1=54.4),

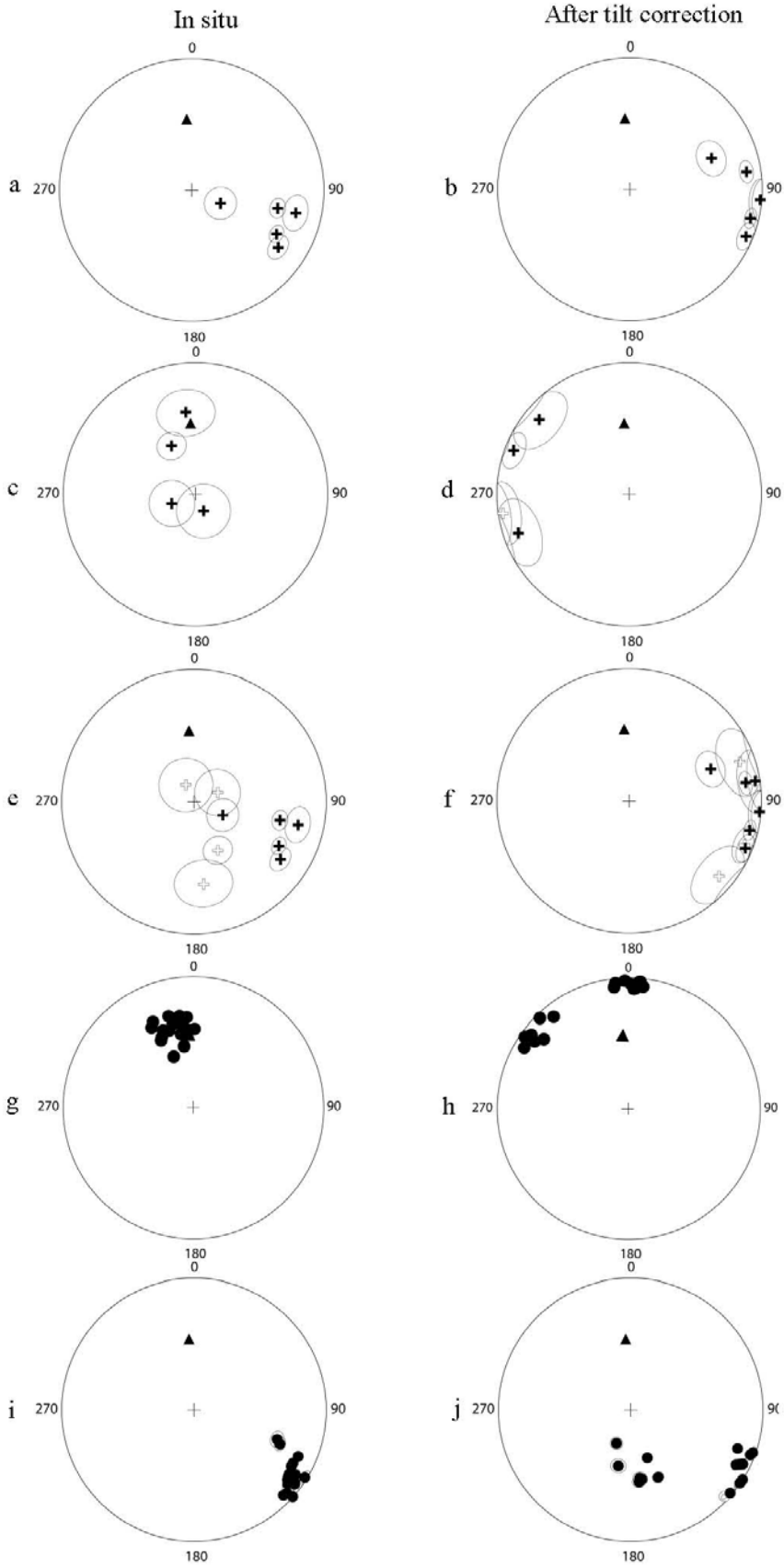

Figure 8. Stereograms of sample-mean directions, in situ and after tilt correction of high- (+) and medium-temperature (●) components. (▲) Present-day geomagnetic field. Sites: a, b, Ait-Abdallah 2; c, d, Ait-Abdallah 4; e, f, Mixing of Ait Abdallah 2 and 4; g, h, medium-temperature of Ait-Abdallah 2 and 4. The high-temperature component better cluster after tilt correction when considering sample-mean rather that mixed directions. The medium-temperature component better cluster for in-situ directions than tilt corrected directions considering mixed sites.

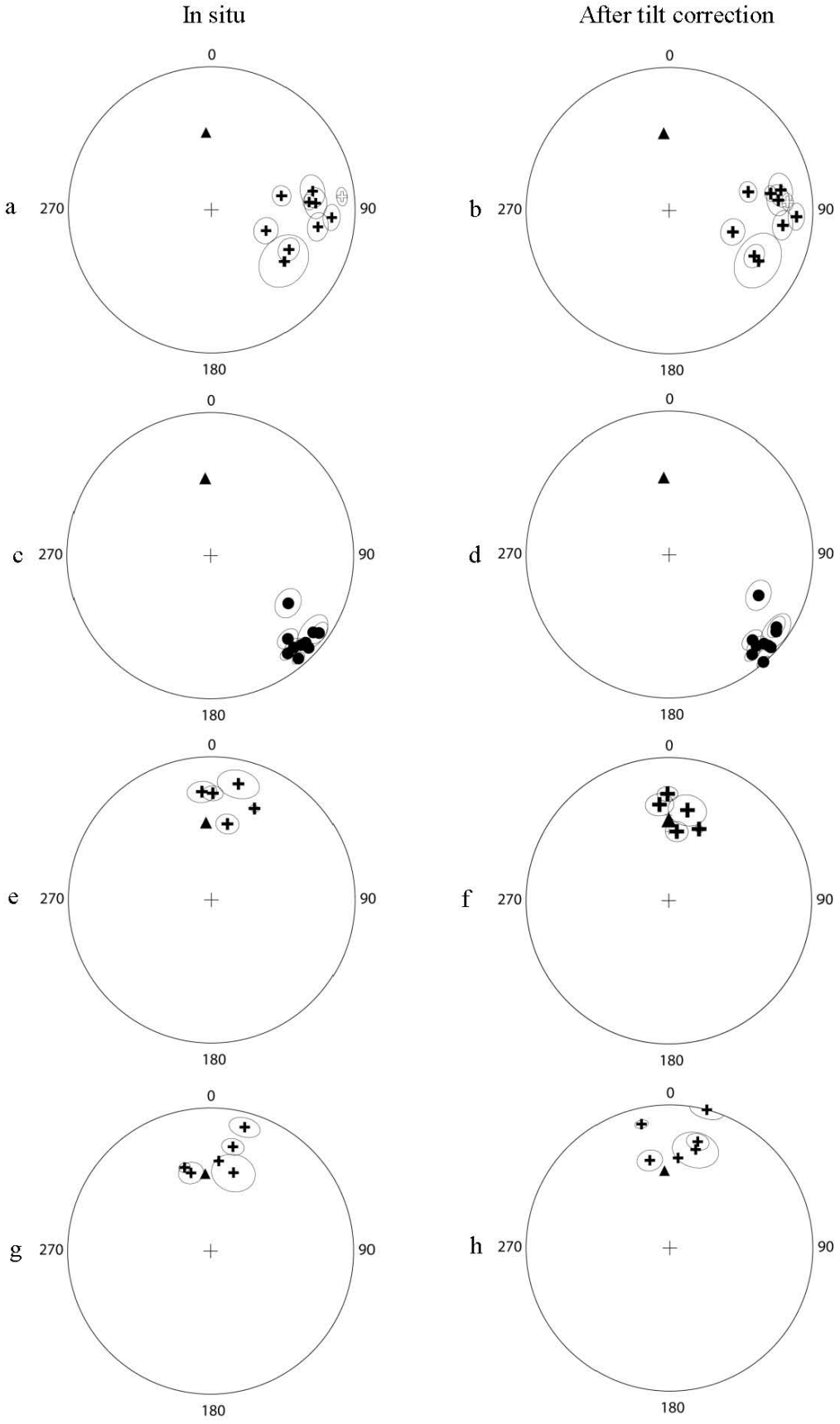

Figure 9. Stereograms of sample-mean directions in situ and after tilt correction of the high- (+) and medium-temperature (●) components. (▲) Present-day geomagnetic field. Sites: a, b, Ida Ougnidif; c, d, medium-temperature components of Ida Ougnidif; e, f, Anfeg; g, h, Douar Tizirt. The precision parameters (k) of the high-temperature component in situ (k_1) and after tilt correction (k_2) are similar within the different sites.

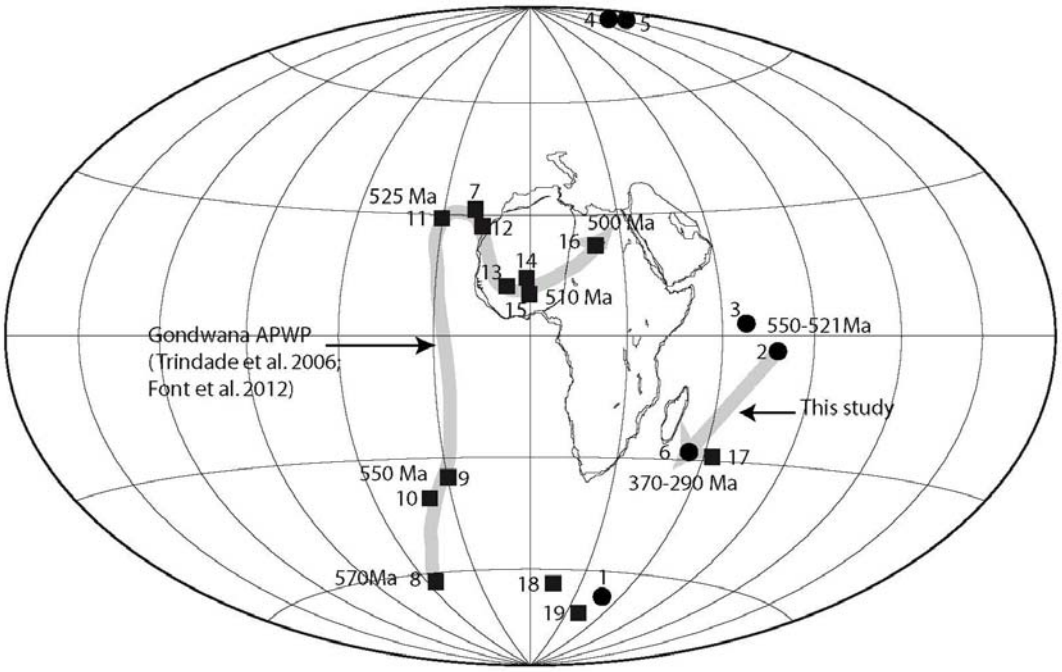

Figure 10. Virtual Magnetic Poles in the Anti-Atlas in Hammer-Aitoff's projection compared with Gondwana APWP (Trindade *et al.* 2006, Font *et al.* 2012) and Permian magnetization (Opdyke *et al.* 2001, Tomezzoli, 2009). (●) This study: 1, mean pole from high-temperature component of Ait-Abdallah 1and 3; 2, mean pole from high-temperature component of Ait-Abdallah 2 and 4; 3, Ida Ougnidif high-temperature pole; 4, Anfeg high temperature component; 5, Douar Tizirt high-temperature component; 6, mean pole from medium-temperature component at Ait-Abdallah 2 and 4 and Ida Ougnidif; (■) From literature: 7, Adma diorite (Morel 1981) ; 8, Nola dolerite (Moloto-A-Kenguemba *et al.* 2010); 9, Mirbat SS (Kempf *et al.* 2000); 10, Sinyai dolerite (Meert & Van der Voo 1996); 11, Itabaiana dikes (Trindade *et al.* 2006); 12, Ntonya Ring (Briden *et al.* 1993); 13, Madagascar virgation (Meert *et al.* 2003); 14, Juiz de Fora Complex (D'Agrella-Filho *et al.* 2004); 15, Carion Granite (Meert *et al.* 2001); 16, Piquete Formation (D'Agrella-Filho *et al.* 1986); 17, Dwyka diamictite (Opdyke *et al.* 2001); 18, Early Permian (Tomezzoli 2009); 19, Late Permian (Tomezzoli 2009).

higher than the precision parameter (k_2=5.6) after tilt-correction, which shows that the magnetization is not primary. The high-temperature components in the limestone of the Ait-Abdallah sites 1 and 3 (Fig. 7e,f) are clearly representative of the present-day field. On the other hand, the high-temperature (500°C to 670°C) component in the siltstone at the Ait-Abdallah 2 and 4 and Ida Ougnidif sites shows easterly magnetization (Figs 8f, 9a,b). In the mean Ait-Abdalllah 2 and 4 (Fig. 8f) this direction, validated by McFadden's (1990) statistics fold test based on very low quantity of processed samples, is considered here as a Permian overprint.

The two Permian directions from medium and high temperature components are associated to the two Hercynian phases of deformation described in the Anti-Atlas (Charlot 1976, Bonhomme & Hassenforder 1985, Sebti *et al.* 2009).

The Virtual Geomagnetic Poles for the high and medium-temperature components from the different sites (Tab. I) are plotted on Hammer-Aitoff's projection together with the present day outline of the African continent (Fig. 10). These poles are compared with the Neoproterozoic-Cambrian and Permian (Tab. II) ones from Africa and South America that are used in GondwanaAPWP (Trindade et *al.* 2006, Font *et al.* 2012).

The mean Ait-Abdallah 2 and 4 high-temperature components give a Virtual Geomagnetic Pole (VGP) at Plon=69.5°, Plat=-28.8°, in situ and Plon=77.7°, Plat=-3.7°, dp=8.2°, dm=16.5°, after tilt correction. The Ida Ougnidif site yields a Virtual Geomagnetic Pole with mean trend Plon=67.3°, Plat=3.4°, dp=8.4°, dm=15.6° which is close to that at the mean Ait-Abdallah sites 2 and 4. The two sites give average Plon=72.5°, Plat=1.2°, dp=6.1°, dm=11.9°. Plotted on Gondwana APWP (Fig. 10) of Africa and Central South America (Trindade *et al.* 2006, Font *et al.* 2012), this paleopole is not close to the 525-550 Ma segment of this APWP corresponding to the age of the Adoudounian Formation dated by U-Pb zircon between 550±3 Ma and 521±7 Ma (Gasquet *et al.* 2005), 534 ± 10 Ma (Alvaro *et al.* 2006) and 524.84 ± 0.09 Ma (Maloof *et al.* 2010). This paleopole corresponds to the one of the Permian remagnetization. The paleopole calculated from the medium-temperature component directions from the Ait-Abdallah 2 and 4 and Ida Ougnidif sites gives Plon=54.9°, Plat=27.8°, dp=2.1°, dm=4.1°. It also corresponds to the direction of Permian remagnetization. These Permian overprints in the Adoudounian Formation were acquired during the Hercynian orogeny dated by Rb-Sr and K-Ar methods on fine illite fractions at around 315-250 Ma (Charlot 1976), 370-290 Ma (Bonhomme & Hassenforder 1985), and at 328±30 Ma (Sebti *et al.* 2009), which was responsible for the folded Anti-Atlas chain. This

Table II. Virtual Geomagnetic Poles of Gondwana APWP of Africa and central South America (Trindade *et al.* 2006, Font *et al.* 2012) and Permian magnetization (Opdyke *et al.* 2001, Tomezzoli, 2009).

Formation	Age (Ma)	Virtual geomagnetic pole		Reference
		Long(°)	Lat(°)	
Adma diorite (WA)	615	341	31	1
Nola dolerite (CA)	570	304.8	–61.8	2
Mirbat SS (AR)	550	330	–34	3
Sinyai dolerite (AR)	547	321	−40	4
Itabaiana dikes (SA)	525	330	29	5
Ntonya Ring (AR)	522	345	28	6
Madagascar virgation (MA)	521	350	13	7
Juiz de Fora Complex (SA)	510	357	10	8
Carion Granite (MA)	508	358	14	9
Piquete Formation (SA)	500	22	24	10
Dwyka diamictite (SAf)	Permian	69.7	–39.7	11
	Early Permian	14	–64	12
	Late Permian	39	–72	12

Data Sources: 1, Morel (1981); 2, Moloto-A-Kenguemba *et al.* (2010); 3, Kempf *et al.* (2000); 4, Meert & Van der Voo (1996); 5, Trindade *et al.* (2006); 6, Briden *et al.* (1993); 7, Meert *et al*. (2003); 8, D'Agrella-Filho *et al.* (2004); 9, Meert *et al.* (2001); 10, D'Agrella-Filho *et al.* (1986); 11, Opdyke *et al.* (2001); 12, Tomezzoli (2009). WA : West Africa ; CA : Central Africa ; AR : Arabia Nubia ; SA : South America ; MA: Madagascar ; SAf: South Africa.

Permian paleopole calculated from the medium-temperature component and which is close to the Permian magnetization of Dwyka diamictite in South Africa (Opdyke *et al.* 2001) is largely different of the Early and Late Permian poles of Tomezzoli (2009). Nevertheless the latter pole is close to the mean Ait-Abdallah 1 and 3 medium-temperature paleopole.

CONCLUSION

The paleomagnetic study of the Adoudounian Formation clearly shows that the sites have recorded later magnetic overprints. The low-temperature component is similar to the present-day field and is probably a viscous remanent magnetization. The high and medium-temperature components record two directions similar to the Permian magnetic field. These overprints are interpreted to result from the Hercynian orogeny that affected the Neoproterozoic and Cambrian rocks of the Anti-Atlas. The high-temperature components are carried by magnetite or the titanohematite or the mixture of the two minerals. The Virtual Geomagnetic Poles corresponding to the mean direction respectively of the high and medium-temperature components at Ait Abdallah site 2-4 and Ida Ougnidif dated Neoproterozoic-Cambrian age are situated in the easterly position compared with the Gondwana pole of the same age. These VGP close to the Permian paleopole are considered here as Permian overprints associated to Hercynian orogeny which was responsible for the folded Anti-Atlas chain. These data show that Permian overprints largely affect the Moroccan Anti-Atlas.

Acknowledgements

The authors would like to acknowledge the ''Centre Européen de Recherches et d'Enseignement des Geosciences de l'Environnement'' (CEREGE). Eric Font (University of Lisbon) and an anonymous reviewer are acknowledged for their reviews. A.C. Maloof and M.O. de Kock are also acknowledged for their contribution to the improvement of the first draft of the manuscript.

References

Alvaro J.J., Ezzouhairi H., Vennin E., Ribeiro M.L., Clausen S., Charif A., Ait Ayad N & Moreira M.E. 2006. The Early-Cambrian Boho volcano of the El Graara massif, Morocco: Petrology, geodynamic setting and coeval sedimentation. *J. Afr. Earth Sci*., 44, 396-410.

Barbey P., Oberli F., Burg J.-P., Nachit H., Pons J & Meier M. 2004. The Palaeoproterozoic in western Anti-Atlas (Morocco): a clarification. *J. Afr. Earth Sci.,* 39 239–245

Bonhomme M.G. & Hassenforder B. 1985. Le métamorphisme hercynien dans les formations tardi et post-panafricaines de l'Anti-Atlas occidental (Maroc); données isotopiques Rb/Sr et K/Ar des fractions fines. *Sci. Géol. Bull.*, 38, 175-183.

Boudzoumou F., Vandamme D., Affaton P., & Gattacceca J., 2010. Palaeomagnetism of Neoproterozoic formations in the Volta basin. *Glob. J. Sci.*, 8, 1, 91-102.

Boudzoumou F., Vandamme D., Affaton P., & Gattacceca J., 2011. Neoproterozoic paleomagnetic poles in the Taoudeni basin (West Africa). *C. R. Geosci.,* 343, 284-294.

Briden J.C., McClelland E. & Rex D. C. 1993. Proving the age of a paleomagnetic pole: the case of the Ntonya Ring structure, Malawi. *J. Geophys. Res.*, 98, 1743-1749.

Charlot R. 1976. The Precambrian of the Anti-Atlas (Morocco): a geochronological synthesis. *Precambr. Res.,* 3, 273-299.

Cogné J.P. 2003. Paleomac: a Macintosh™ application for treating paleomagnetic data and making plate reconstruction. *Geochem. Geophys. Geosyst.,* 4, 1007.

D'Agrella-Filho M.S., Pacca I. & Sato K. 1986. Paleomagnetism of metamorphic rocks from the Piquete Region-Ribeira Valley, Southeastern Brazil. *Rev. Bras. Geofıs.,* 4, 79-84.

D'Agrella-Filho M.S., Raposo M.I.B. & Egydio- Silva M. 2004. Paleomagnetic Study of the Juiz de Fora Complex, SE Brazil: implications for Gondwana. *Gondwana Res.,* 7, 103-113.

Day R., Fuller M.D. & Schmidt V.A. 1977. Hysteresis properties of titanomagnétites: grain size and composition dependence. *Phys. Earth Planet. Int.,* 13, 260-267.

Fischer R.A. 1953. Dispersion on a sphere. *Proc. R. Soc. Lond.,* A 217. 295-305.

Font E., Rapalini A.E., Tomozzoli R.N., Trindade R.I.F. & Tohver E. 2012. Episodic remagnetizations related to tectonic events and their consequences for the South America Polar Wander Path. *In*: Elmore R.D., Muxworthy, A.R., Aldana M.M. & Mena M. (eds) - Remagnetization and Chemical Alteration of Sedimentary Rocks. *Geol. Soc, Lond.,* sp. pub 371, 55-87.

Gasquet D., Levresse G., Cheilletz A., Azizi-Samir M.R. & Mouttaqi A. 2005. Contribution to a geodynamic reconstruction of the Anti-Atlas (Morocco) during Pan-African times with the emphasis on inversion tectonics and metallogenic activity at the Precambrian–Cambrian transition. *Precambr. Res.,* 140, 157-182.

Inglis J.D., MacLean J.S., Samson S.D., D'Lemos R.S., Admou H. & Hefferan K. 2004. A precise U–Pb zircon age for the Bleïda granodiorite, Anti-Atlas, Morocco: implications for the timing of deformation and terrane assembly in the eastern Anti-Atlas. *J. Afr. Earth Sci.,* 39, 277-283.

Kempf O., Kellerhals P., Lowrie W. & Matter A. 2000. Paleomagnetic directions in Late Precambrian glaciomarine sediments of the Mirbat Sandstone Formation, Oman. *Earth Planet. Sci. Lett.,* 175, 181-190.

Kirschvink J.L. 1980. The least-squares lines and plane and the analysis of paleomagnetic data. *Geophys. J. R. Astron. Soc.,* 62, 699-718.

Lowrie W. 1990. Identification of ferromagnetic minerals in a rock by coercivity and unblocking temperature properties. *Geophys. Res. Lett.,* 17, 159-162.

Malek H.A., Gasquet D., Bertrand J.M. & Leterrier J. 1998. Géochronologie U-Pb sur zircon de granitoïdes éburnéens et panafricains dans les boutonnières protérozoïques d'lgherm, du Kerdous et du Bas Drâa (Anti-Atlas occidental, Maroc). *C.R. Acad. Sci.,* 327, 819-826.

Maloof A.C., Ramezani J, Bowring S.A., David A. Fike D.A., Susannah M., Porter S.M. & Mohamed Mazouad M. 2010. Constraints on early Cambrian carbon cycling from the duration of the Nemakit-Daldynian–Tommotian boundary $\delta^{13}C$ shift, Morocco. *Geol. Soc. Amer.,* 38, 7, 623-626.

McFadden P.L. 1990. A new fold test for paleomagnetic studies. *Geophys. J. Int.,* 103, 163-169.

Meert J.G. & Van der Voo, R. 1996. Paleomagnetic and $^{40}Ar/^{39}Ar$ study of the Sinyai dolerite, Kenya: implications for Gondwana assembly. *J. Geol.,* 104, 131-142.

Meert J.G., Nédélec A. & Hall C. 2003. The stratoid granites of central Madagascar: paleomagnetism and further age constraints on Neoproterozoic deformation, *Precambr. Res.,* 120, 101-129.

Meert J.G., Nédélec A., Hall C.,Wingate M.T.D. & Rakotondrazafy M. 2001. Paleomagnetism, geochronology and tectonic implications of the Cambrian-age Carion granite, Central Madagascar. *Tectonophys.*, 340, 1-21.

Moloto-A-Kenguemba G.R., Trindade R.I.F., Monié P., Nédélec A. & Siqueira R. 2008. A late Neoproterozoic paleomagnetic pole for the Congo craton: tectonic setting, paleomagnetism and geochronology of the Nola dike swarm (Central African Republic). *Precambr. Res.,* 164, 214-226.

Morel P. 1981. Palaeomagnetism of a Pan-African diorite: a late Precambrian pole for western Africa. *Geophys. J. Royal Astr. Soc.,* 65, 493-503.

Mortaji A., Ikenne M., Gasquet D., Barbey P. & Stussi J.M. 2000. Les granitoïdes paléoprotérozoïques des boutonnières du Bas Drâa et de la Tagragra d'Akka (Anti-Atlas occidental, Maroc) : un élément du puzzle géodynamique du craton ouest-Africain. *J. Afr. Earth Sci.,* 31, 523-538.

Opdyke N.D., Mushayandebvu M., & Dewit M.J. 2001. A new palaeomagnetic pole for the Dwyka System and correlative sediments in sub-Saharan Africa. *J. Afr.Earth Sci.,* 33, 143-153.

Sebti S., Saddiqi O., El Haimer F.Z., Michard A., Ruiz G., Bousquet R., Baidder L. & Frizon de Lamotte D. 2009. Vertical movements at the fringe of the West African Craton: first zircon fission track datings from the Anti-Atlas Precambrian basement, Morocco. *C. R. Geosci.,* 341, 71-77.

Tauxe L. 2009. Essentials of Paleomagnetism: Web Edit., 1.0 March 18.

Thomas R.J., Chevallier L.P., Gresse P.G., Harmer R.E., Eglington B.M., Armstrong R.A., De Beer C.H., Martini J.E.J., De Kock G.S., Macey P.H. & Ingram B.A. 2002. Precambrian evolution of the Sirwa Window, Anti-Atlas Orogen, Morocco, *Precambr. Res.,* 118, 1-57.

Tohver E., D'Agrella-Filho M.S. & Trindade R.I.F. 2006. Paleomagnetic record of Africa and South America for the 1200-500 Ma interval, and evaluation of Rodinia and Gondwana assemblies. *Precambr Res.,* 147, 193-222.

Tomezzoli R.N. 2009. The apparent polar wander path for South America during the Permian–Triassic. *Gondwana Res.,* 15, 209-215.

Trindade R.I.F., D'Agrella-Filho M.S., Epof I. & Brito Neves B.B. 2006. Paleomagnetism of early Cambrian Itabaiana mafic dikes (NE Brazil) and the final assembly of Gondwana. *Earth Planet. Sci. Lett.,* 244, 361-377.

Zijderveld J.D.A. 1967. AC demagnetization of rocks: Analysis of result. *In*: Collinson D.W., Runcorn S.K., Creer K.M. (eds.) - *Methods in Paleomagnetism*. Elsevier New York, 254-286.

Manuscript received 4 april 2012
Revised version accepted 30 november 2012